ARTICLE

Check for updates

Multivariate relationships between social cognitive performance and functional connectivity during task and rest across schizophrenia spectrum disorders and healthy controls

Lindsay D. Oliver[1,2], Ju-Chi Yu[1], Colin Hawco[1,2], Navona Calarco[1,3,4], Vinh Tan[1,5], Iska Moxon-Emre[1], Sunny X. Tang[6,7,8], James M. Gold[9], George Foussias[1,2], Pamela DeRosse[10], Miklos Argyelan[6,7,8], Robert W. Buchanan[9], Anil K. Malhotra[6,7,8], Aristotle N. Voineskos[1,2]✉and the SPINS Group*

Social cognitive deficits are common and impact functional outcomes in people with schizophrenia spectrum disorders (SSDs). Functional brain networks during task and rest show complex relationships with cognition. We aimed to identify relationships between social and non-social cognitive performance and functional connectivity during social processing and at rest across individuals with SSDs and healthy controls. Adults ($N = 352$; 195 SSDs, 157 controls) completed functional magnetic resonance imaging (fMRI) during the Empathic Accuracy (EA) task and rest, and cognitive assessments. Partial least squares correlation was used to identify latent dimensions (LDs) capturing multivariate relationships between functional connectivity and cognitive measures, evaluated using permutation testing, bootstrapping, and cross-validation. Two significant EA LDs were identified, explaining 73.6 and 9.1% of the variance. EA LD1 captured an association between better performance across cognitive measures and positive connectivity across networks implicated in processing dynamic multimodal and social stimuli. EA LD2 reflected an association between worse EA task performance and stronger positive connectivity between networks implicated in language and social processing. One significant resting-state LD was identified, explaining 85.6% of the variance and capturing an association between better overall cognition and visual, somatomotor, and subcortical connectivity, driven more by the SSD group. Overlapping and divergent connectivity patterns appear to covary with cognitive performance during social processing versus rest across SSDs and healthy controls. Our results support the value of task-based fMRI to identify dimensional functional connectivity patterns associated with particular social cognitive abilities, whereas resting-state connectivity may reflect broader relationships with cognition.

Molecular Psychiatry; https://doi.org/10.1038/s41380-026-03504-8

INTRODUCTION

People with schizophrenia spectrum disorders (SSDs) often exhibit social cognitive deficits, which contribute to disability and poor functional outcomes [1, 2]. Impairments in both lower-level 'simulation' (e.g., emotion processing) and higher-level 'mentalizing' (e.g., theory of mind) processes [3], as well as non-social cognition (e.g., processing speed, working memory) [4], have been consistently observed in SSD versus healthy control groups [5]. Social cognitive deficits, and particularly higher-level mentalizing, are also often related to non-social cognition in people with SSDs, though evidence suggests these are distinct domains [6, 7]. Both social and non-social cognition have been identified as promising treatment targets in SSDs given their links with functional outcomes [5, 8, 9]. However, meta-analyses indicate that social cognition shows a stronger relationship with functioning than non-social cognition [8] and may mediate the effect of non-social cognition on functional outcomes [9], highlighting the potential value of targeting social cognitive deficits and the importance of delineating underlying neural mechanisms to guide treatment development.

Reduced activation [10–12] and connectivity differences [13, 14] during social cognitive tasks have been reported in regions of a lower-level frontoparietal and insular 'simulation network' [15, 16] and a higher-level cortical midline and lateral temporal 'mentalizing network' [17, 18] in people with SSDs compared to healthy controls. These networks show overlap with the resting-state frontoparietal and cingulo-opercular/salience networks, and the default (mode) network, respectively [19]. Resting-state functional

[1]Campbell Family Mental Health Research Institute, Centre for Addiction and Mental Health, Toronto, ON, Canada. [2]Department of Psychiatry, University of Toronto, Toronto, ON, Canada. [3]Department of Medical Biophysics, University of Toronto, Toronto, ON, Canada. [4]Krembil Brain Institute Institute, Toronto Western Hospital, Toronto, ON, Canada. [5]Institute of Medical Science, University of Toronto, Toronto, ON, Canada. [6]Division of Psychiatry Research, The Zucker Hillside Hospital, Division of Northwell Health, Glen Oaks, NY, USA. [7]The Donald and Barbara Zucker School of Medicine at Hofstra/Northwell, Department of Psychiatry, Hempstead, NY, USA. [8]Center for Psychiatric Neuroscience, The Feinstein Institute for Medical Research, Manhasset, NY, USA. [9]Maryland Psychiatric Research Center, Department of Psychiatry, University of Maryland School of Medicine, Baltimore, MD, USA. [10]Department of Psychology, Stony Brook University, Stony Brook, NY, USA. *A list of authors and their affiliations appears at the end of the paper. ✉email: aristotle.voineskos@camh.ca

Received: 23 January 2025 Revised: 20 January 2026 Accepted: 18 February 2026
Published online: 12 March 2026

magnetic resonance imaging (fMRI) has been proposed as a context-independent means of examining the neural correlates of social processing [20], given the overlap between default network regions engaged during rest (i.e., unconstrained cognition) and social cognition [21, 22]. Though resting-state functional connectivity has been associated with social cognitive performance in smaller SSD samples [23–26], it has also been linked to non-social cognitive performance across multiple studies in SSDs [27] and other behavioral and clinical metrics in transdiagnostic samples [28–30]. We previously found that resting-state functional connectivity was able to distinguish between participant clusters across SSDs and healthy controls with differing cognitive performance and functioning profiles [31].

However, the continued dominance of resting-state fMRI data collection has been a topic of recent debate, particularly for the examination of brain-behavior relationships [32], given that naturalistic viewing and task-based fMRI have shown increased sensitivity to these relationships [33, 34] and enhance interpretability of findings [32]. Neural activation [10, 35] and functional connectivity [14, 36–38] patterns during social cognitive task-based fMRI have been associated with social cognitive performance in people with SSDs, though region and directionality have varied and sample sizes have tended to be smaller. Recent work from our group across a large sample of people with SSDs and healthy controls using the social processing Empathic Accuracy (EA) task [39, 40] found that greater segregation (i.e., less positive and greater negative connectivity) between social cognitive networks was related to better social cognitive performance, irrespective of diagnostic group; however, this univariate analysis examined only cortical social cognitive networks and social cognitive performance metrics [41]. Despite increasing knowledge regarding the neural underpinnings of social cognitive impairments, functional brain networks have complex and overlapping relationships, as do cognitive tasks.

The present study uniquely leverages a comprehensive social and non-social cognitive battery and both social task-based and resting-state fMRI data across a large sample of individuals with SSDs and healthy controls, to better understand how functional brain networks engaged during social processing versus rest relate to performance across cognitive domains. We used partial least squares correlation (PLSC) to examine data-driven multivariate relationships between cognitive performance measures and functional connectivity across cortical and subcortical brain regions both during the EA task and at rest. Relationships between significant behavior and functional brain pattern scores and diagnostic group were examined, as well as sex, age, and motion during scanning. We hypothesized that functional connectivity during social processing, particularly of the frontoparietal, cingulo-opercular, and default networks that show overlap with social cognitive networks, would covary with social cognitive behavioral domains, perhaps reflecting the delineation of lower- and higher-level social cognitive and non-social cognitive constructs. In contrast, resting-state data may reveal more general associations between functional connectivity across a broader set of networks and cognition across domains.

MATERIALS AND METHODS

Participants

Participants aged 18–59 were recruited for the Social Processes Initiative in the Neurobiology of the Schizophrenia(s) (SPINS) study from the Centre for Addiction and Mental Health (CAMH; Toronto, Canada), Zucker Hillside Hospital (ZHH; New York, USA), and the Maryland Psychiatric Research Center (MPRC; Maryland, USA) between 2014–2020. Of 300 participants with a SSD and 185 healthy individuals who maintained eligibility requirements ($N = 485$), 195 participants with a SSD and 157 healthy controls ($N_2 = 352$; mean (SD) age=32 (10); 216 males, 136 females) were included in data analyses following quality control (see Figure S1). Participants with SSDs met DSM-5 diagnostic criteria for schizophrenia, schizoaffective disorder, schizophreniform disorder, delusional disorder, or psychotic disorder not otherwise specified, assessed using the Structured Clinical Interview for DSM (SCID-IV-TR), and had no change in antipsychotic medication or decrement in functioning/support level in the 30 days prior to enrollment. Healthy control participants did not have a current or past Axis I psychiatric disorder, excepting adjustment disorder, phobic disorder, and past major depressive disorder (over two years prior; presently unmedicated), or a first degree relative with a history of psychotic mental disorder. Additional exclusion criteria included a history of head trauma resulting in unconsciousness, a substance use disorder (confirmed by urine toxicology screening), intellectual disability, debilitating or unstable medical illness, or other neurological diseases. Participants also had normal or corrected-to-normal vision. Chlorpromazine (CPZ) equivalents were calculated for the SSD group based on collected medication information using the R package chlorpromazineR [42, 43]. All participants signed an informed consent agreement and the protocol was approved by the respective research ethics and institutional review boards at CAMH, ZHH, and MPRC. All research was conducted in accordance with the Declaration of Helsinki.

Clinical and cognitive assessment

Data collection occurred across three visits (Visit 1: Consent, screening, clinical scales; Visit 2: MRI; Visit 3: Social and non-social cognitive testing).

All participants completed the Wechsler Test of Adult Reading to screen for premorbid IQ. Psychiatric symptoms were assessed in the SSD sample only using the Brief Psychiatric Rating Scale (BPRS) and the Scale for the Assessment of Negative Symptoms (SANS). Functioning was evaluated using the Birchwood Social Functioning Scale (BSFS) across groups, and the Quality of Life Scale (QLS) in the SSD group only.

Social cognitive tasks ranged from basic emotion recognition to complex mental state inference, and were selected based on findings from the Social Cognition Psychometric Evaluation (SCOPE) study [44] and the Social Cognition and Functioning in Schizophrenia project [39]. These included the Penn Emotion Recognition Test (ER40 [45]), which assesses basic emotion recognition from static images, the Reading the Mind in the Eyes test (RMET [46]), involving mental state recognition from the eye region of faces, and the Empathic Accuracy (EA) task, which was completed during fMRI [39, 40]. Participants also completed The Awareness of Social Inference Test - Revised (TASIT [47]), which involves viewing social video clips and includes three subtests (TASIT 1: Identifying emotions; TASIT 2 and 3: Social inference, including detection of lies and sarcasm).

Non-social cognition was evaluated using the MATRICS (Measurement and Treatment Research to Improve Cognition in Schizophrenia) Consensus Cognitive Battery (MCCB [48]), which includes domain scores for processing speed, reasoning and problem solving, attention/vigilance, working memory, verbal learning, and visual learning. For participants missing only one cognitive measure of interest, data were imputed using the mice package in R ($N = 9$; see Supplementary Material).

Empathic accuracy (EA) task

The EA task [39, 40] consists of nine videos (110–180 s each), presented in three runs (~9 mins/run), of individuals describing emotional autobiographical events. Throughout the videos, participants provide continuous ratings of how positive or negative the individual in the video is feeling. EA was calculated for each participant by correlating their ratings with self-ratings provided by the individuals in the videos (see Supplementary Material). The EA task is a more naturalistic social cognitive task given that it is dynamic and multimodal, and it engages regions spanning both simulation and mentalizing social cognitive networks [49–51], making it effective for exploring their interaction [41].

MRI data acquisition

MRI scans were collected using harmonized scanning parameters and standardized operating procedures on six 3 T scanners with multichannel head coils (see Supplementary Material for details and scanning parameters). The anatomical scan(s), resting-state scan, and EA task were part of a longer multimodal MRI protocol, as previously described [31].

MRI quality control

Prior to analyses, all scans were quality checked by experienced research staff before and after preprocessing. Participants were also excluded for excessive motion (mean framewise displacement (FD) > 0.5 mm) and for EA or control task performance indicative of disengagement or a lack of comprehension (see Supplementary Material and Figure S1).

MRI preprocessing

MRI preprocessing was performed using fMRIPrep 1.5.8 [52] (see Supplementary Material for details). Anatomical T1-weighted images were corrected for intensity non-uniformity and skull-stripped [53], followed by brain tissue segmentation [54], normalization to MNI space using nonlinear registration, and brain surface reconstruction [55]. Functional data underwent slice-timing correction [56], motion correction [57], and fieldmap-less distortion correction [58], and was coregistered to the corresponding T1-weighted image.

The Ciftify toolbox (https:// github.com/edickie/ciftify [59]) was then used to project the functional data onto the cortical surface, drop four TRs for each EA scan and three TRs for the resting-state scan, and smooth the functional data using a 2 mm full width at half maximum Gaussian kernel. For resting-state data, detrending, band-pass filtering (0.01–0.1 Hz), and nuisance regression were also performed using Ciftify. For the EA task data, detrending and nuisance regression occurred within the GLM. For both EA and resting-state data, the nuisance regression model included the six head motion correction parameters, mean white matter signal, and mean cerebral spinal fluid signal, and the square, derivative, and square of the derivative for each of these regressors.

An amplitude modulated GLM was used to model the EA task with AFNI's 3dDeconvolve module in Nipype [60]. For each of the nine EA videos, one hemodynamic response function (HRF) was fit for the duration of the video, as well as a second HRF modulated by the participant's EA score, and a third HRF was fit for button presses made during the EA videos (duration 1 s). Control videos were also modeled, including one HRF for the duration of the video and a second HRF for button presses made during the video (duration 1 s). These regressors were fit to each voxel to model the stimulus-evoked response, and the residual activation was retained for background connectivity analysis.

Connectivity matrix construction

Functional connectivity during the EA task was analyzed using background connectivity, which removes the modeled stimulus-evoked response and correlates residual activation over time across regions of interest. Thus, the focus is on state-related functional connectivity rather than stimulus-driven coactivation [61, 62]. This is ideal for continuous tasks, and the EA task in particular, given that we were interested in the state of emotional understanding across videos rather than individual responses to video events. This approach also aligns well with resting-state functional connectivity analyses.

For connectivity matrix construction, the brain was parcellated using the cortical Multimodal Parcellation (MMP) 1.0 atlas (360 regions [63]) and the Melbourne Subcortex Atlas (Scale II; 32 regions [64]). For visualization and interpretation purposes, twelve resting-state cortical networks were defined based on the Cole-Anticevic Brain Network Parcellation [65], with the subcortical regions grouped separately. A mean time series was extracted for each of the 392 regions for both resting-state and EA residual data. For the EA task, control videos were removed from the time series data prior to generating connectivity matrices. Pearson correlation coefficients were calculated between the time courses of each pair of regions and Fisher's *Z*-transformed, generating 392×392 EA and resting-state connectivity matrices for each participant. Functional connectivity data was harmonized across the six MRI scanners using ComBat, a batch-effect correction tool, via the neuroCombat package in R ([66]; see Supplementary Material).

STATISTICAL ANALYSES

Data were analyzed using RStudio Version 1.4.1717 [67] and the TExPosition package [68]. Partial least squares correlation (PLSC) was used to identify latent dimensions (LDs) that capture multivariate brain-behavior relationships. Each LD is composed of a brain (derived from functional connectivity) and behavior (derived from cognitive measures) latent variable pair that has the maximal covariance, where all LDs have covariance in a descending order [69]. As in recent work [38, 70, 71], we reduced the dimensionality of the connectivity data by retaining the top ten percent most variable connections defined by median absolute deviation, a measure of variability that is robust to outliers, for each of the EA and resting-state PLSC analyses (see Figure S2). Individual differences cannot be predicted from features that lack variation across participants [71], and prior work from our group using both the EA task and resting-state data from the SPINS sample has shown that connections with the largest deviation are captured in the top ten percent [38]. Thus, the input functional connectivity data included 7664 unique connections and 15 behavioral metrics (nine social cognitive measures: ER40, RMET, EA Task, TASIT 1 Emotion Evaluation, TASIT 2 Sincere, Simple Sarcasm, and Paradoxical Sarcasm, TASIT 3 Lies, and Sarcasm; six non-social cognitive measures from the MCCB: Speed of Processing, Attention/Vigilance, Working Memory, Verbal Learning, Visual Learning, Reasoning and Problem Solving). Variables were centered and scaled (to sum of squares = 1) prior to analyses to ensure comparability and equal contribution. PLSC is well-suited for high-dimensional data analysis in revealing the underlying structure of associations and handling multicollinear features [72]. PLSC performs singular value decomposition on the correlation matrix between two variable sets, producing brain and behavior loadings (or saliences) [73]. Brain and behavior latent variables are linear projections of the original functional connectivity and behavior values onto their respective LDs, with loadings as coefficients [73]. The squared coefficients quantify the variance contributed by each variable to the LD, referred to as contributions, which describe the effect size.

Permutation tests (1000 iterations) were used to evaluate if the identified LDs explained a significant amount of covariance at $\alpha = 0.05$. Effects from the first LD were subtracted from the correlation matrix prior to the permutation test for the second LD [74, 75]. To evaluate the stability of variables' contributions to each LD, a bootstrap procedure (1000 iterations) was used to estimate the bootstrapped confidence intervals and standard deviation of each brain and behavior loading [69, 73]. Bootstrap ratios are then obtained as *Z*-approximates determining whether a given loading is significantly different from 0, where values greater than 2 are considered significant [73]. We used a more stringent threshold of 2.6, corresponding to the critical value of *Z* at $p = 0.01$, given our large number of input variables. Separate PLSC analyses were run using EA and resting-state functional connectivity data to see whether connectivity during social processing might be differentially associated with, or better distinguish between, cognitive performance measures. To examine whether the associations identified by the LDs were driven by a specific group, Pearson's correlations between brain and behavior latent variable scores for each significant LD were computed across all participants and by diagnostic group.

Post-hoc independent *t*-tests were conducted to determine whether brain and behavior latent variable scores for significant LDs differed between participants with SSDs and healthy controls, and by sex assigned at birth. Pearson's correlations were also performed to examine the association between brain and behavior latent variable scores and age and head motion (mean FD), as well as antipsychotic dose (chlorpromazine equivalent (CPZE) milligrams) in SSDs only. False discovery rate (FDR) was used for multiple comparisons correction. The EA and resting-state PLSC models were verified using 10-fold and 4-fold cross-validation, evaluated via correlations between originally observed and predicted latent variable scores and estimated loadings (see Supplementary Material). PLSC was also conducted for EA using only functional connectivity data from the first EA run to evaluate the stability of the EA results and ensure that differential results between EA and resting-state data were not driven by differences in scan length. Lastly, PLSC was performed for EA and resting-state after regressing out age, sex, and mean FD from both functional connectivity and behavioral data.

Code used for these analyses can be found here: https://github.com/loliver4/SPINS_PLS_Conn.

Table 1. Participant demographic information, cognitive scores, and clinical characteristics by diagnostic group.

	SSD ($N = 195$)		Control ($N = 157$)		
	N	%	***N***	%	*p*
Sex at birth (male)	132	67.7	84	53.5	0.009
	Mean	**SD**	**Mean**	**SD**	
Age (years)	31.16	9.42	32.32	10.55	0.280
ER40	32.25	4.44	33.62	3.35	0.001
RMET	25.27	5.04	27.93	3.52	<0.001
Empathic Accuracy (EA)	0.75	0.29	0.89	0.21	<0.001
TASIT 1	22.97	3.24	24.71	2.01	<0.001
TASIT 2 Sincere	17.03	3.06	17.52	2.65	0.109
TASIT 2 Simple Sarcasm	15.56	4.42	18.5	1.8	<0.001
TASIT 2 Paradoxical Sarcasm	16.28	3.39	18.57	2.02	<0.001
TASIT 3 Lie	25.11	4.02	27.27	3.44	<0.001
TASIT 3 Sarcasm	24.07	4.64	27.54	3.63	<0.001
Processing Speed	40.50	12.93	53.45	9.74	<0.001
Attention/Vigilance	40.04	11.24	47.99	12.16	<0.001
Working Memory	41.75	11.12	49.52	11.29	<0.001
Verbal Learning	41.36	9.00	50.62	9.24	<0.001
Visual Learning	39.90	12.09	49.10	9.57	<0.001
Reasoning and Problem Solving	43.71	10.90	49.07	9.31	<0.001
WTAR (standard score)	107.01	14.35	113.6	11.15	<0.001
BPRS Total	31.45	8.00	--	--	--
SANS Total	25.01	12.54	--	--	--
QLS Total	74.44	20.72	--	--	--
BSFS Total	137.45	23.83	175.22	19.39	<0.001

SSD schizophrenia spectrum disorder, *SD* standard deviation, *ER40* penn emotion recognition test, *RMET* reading the mind in the eyes test, *TASIT* the awareness of social inference test - revised, *WTAR* wechsler test of adult reading, *BPRS* brief psychiatric rating scale, *SANS* scale for the assessment of negative symptoms, *QLS* quality of life scale, *BSFS* birchwood social functioning scale; Non-social cognitive measures represent domain scores from the MATRICS.

RESULTS

Participant demographic information, cognitive scores, and clinical characteristics are presented by diagnostic group in Table 1.

Empathic accuracy (EA) results

Two LDs from the EA PLSC survived the permutation test. EA LD1 captured an association between better overall cognitive performance and connectivity patterns across the language, auditory, somatomotor, visual, cingulo-opercular, frontoparietal, and default networks (Fig. 1). This LD accounted for 73.6% of functional connectivity-behavior covariance ($p = 0.001$), with a significant association between EA connectivity and behavior latent variable scores across groups ($r = 0.414$, $p < 0.001$). All social and non-social cognitive metrics were positively associated with the corresponding connectivity patterns, with all but TASIT 2 sincere and TASIT 3 lies having significant and stable loadings (Fig. 1b). Of these, the RMET, TASIT 1, TASIT 2 simple and paradoxical sarcasm, TASIT 3 sarcasm, processing speed, working memory, and verbal and visual learning appeared to be important contributors to EA LD1 (Fig. 1a). These behavioral patterns were associated with increased positive connectivity within the language, auditory, somatomotor, secondary visual, cingulo-opercular, and frontoparietal networks, and between-network connectivity of the language, auditory, posterior-multimodal, cingulo-opercular, frontoparietal, and default networks (positive loadings; Figs. 1c and 1e). Smaller contributions were seen for reduced positive connectivity within and between the default network (including default to frontoparietal and orbito-affective networks), and between the somatomotor and dorsal attention, and language and ventral-multimodal networks (negative loadings; Figs. 1d and 1f), in relation to better cognitive performance.

EA LD2 reflected an association between worse performance on the EA task and increased connectivity between the language, default, cingulo-opercular, and frontoparietal networks (Fig. 2). This LD accounted for 9.1% of brain-behavior covariance ($p = 0.001$), with a significant correlation between EA connectivity and behavior scores across groups ($r = 0.296$, $p < 0.001$). The identified connectivity patterns were associated with generally worse social cognitive performance and improved non-social cognitive performance. Though EA, the RMET, TASIT 2 sincere, TASIT 3 lies, processing speed, and attention/vigilance appeared to be important contributors to LD2 (Fig. 2a), only EA demonstrated significant and stable loadings (Fig. 2b). Worse EA performance was associated with greater positive between-network connectivity of the language, default, cingulo-opercular, frontoparietal, dorsal attention, posterior-multimodal, and primary visual networks, and connectivity within the somatomotor network (positive loadings; Figs. 2c and 2e). Decreased positive connectivity within the language and frontoparietal networks also contributed to LD2 (negative loadings; Figs. 1d and 1f).

EA post-hoc analyses

Examining latent variable score associations for EA LD1 by diagnostic group revealed significant correlations between brain and behavior scores in both SSD ($r = 0.408$, $p < 0.001$, $pFDR < 0.001$) and control ($r = 0.174$, $p = 0.029$, $pFDR = 0.029$) groups. However, diagnostic groups were distinguishable based on EA LD1 (Fig. 3a) as shown by non-overlapping 95% bootstrap

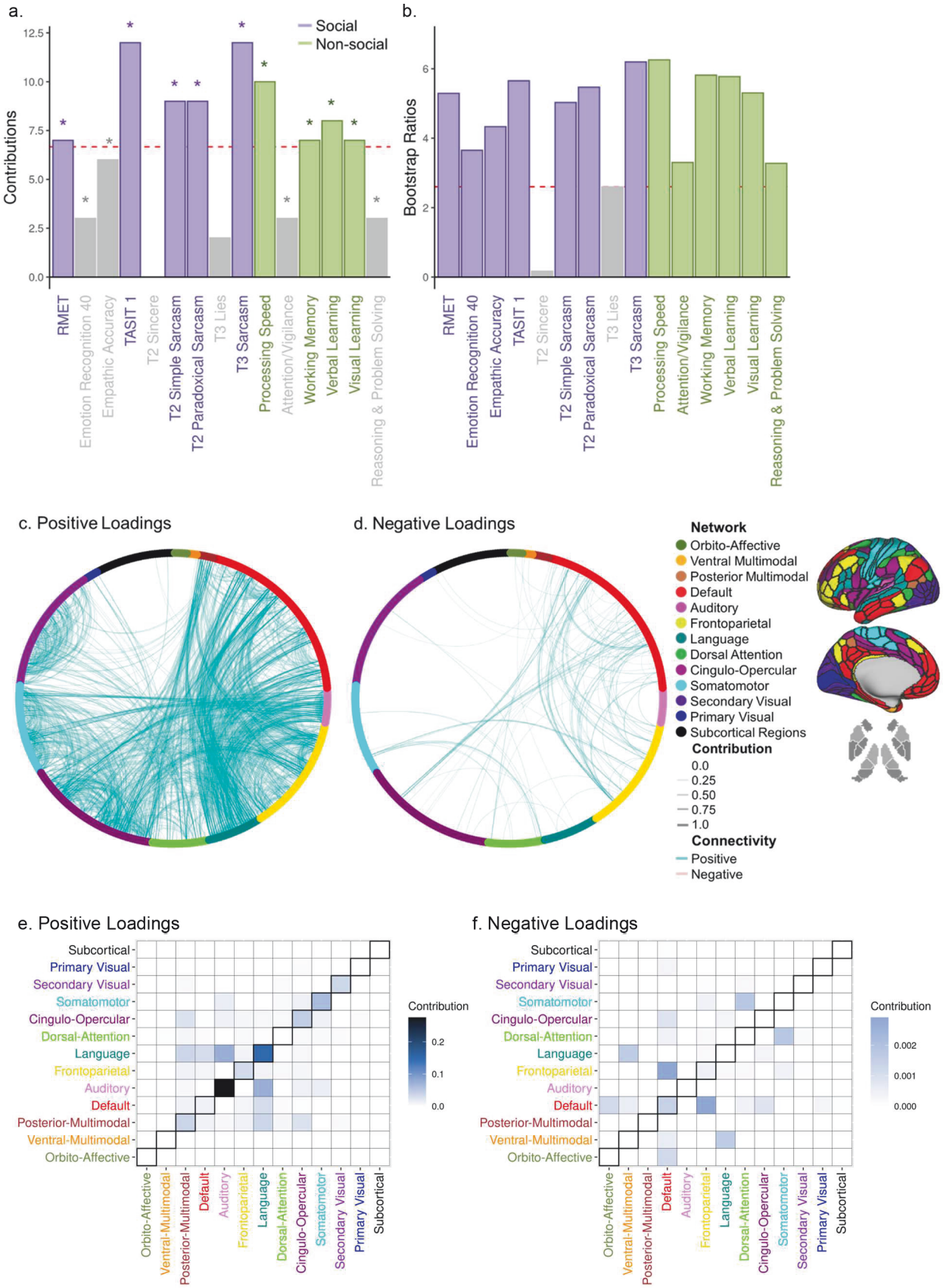
a.
Social
Non-social
Contributions
12.5
10.0
7.5
5.0
2.5
0.0
RMET
Emotion Recognition 40
Empathic Accuracy
TASIT 1
T2 Sincere
T2 Simple Sarcasm
T2 Paradoxical Sarcasm
T3 Lies
T3 Sarcasm
Processing Speed
Attention/Vigilance
Working Memory
Verbal Learning
Visual Learning
Reasoning & Problem Solving
b.
Bootstrap Ratios
6
4
2
0
c. Positive Loadings
d. Negative Loadings
Network
Orbito-Affective
Ventral Multimodal
Posterior Multimodal
Default
Auditory
Frontoparietal
Language
Dorsal Attention
Cingulo-Opercular
Somatomotor
Secondary Visual
Primary Visual
Subcortical Regions
Contribution
0.0
0.25
0.50
0.75
1.0
Connectivity
Positive
Negative
e. Positive Loadings
f. Negative Loadings
Contribution
0.2
0.1
0.0
0.002
0.001
0.000
Subcortical
Primary Visual
Secondary Visual
Somatomotor
Cingulo-Opercular
Dorsal-Attention
Language
Frontoparietal
Auditory
Default
Posterior-Multimodal
Ventral-Multimodal
Orbito-Affective

Fig. 1 EA Latent Dimension (LD) 1. *EA LD1* (**a**) *behavioral effect sizes* (**b**) *and loading stability*. **a** Contributions of behavioral variables for EA LD1. Contributions are calculated as the squared loadings and quantify the amount of variance contributed to the LD by each variable, indicating the effect size. The direction of the contributions reflects the loading direction. Variables with contributions that exceed the dashed line, which represents the average contribution, can be considered important [110]. Asterisks indicate those that were significant and stable according to bootstrap ratios. **b** Bootstrap ratios of behavioral loadings for EA LD1. A bootstrap procedure was used to identify variables with loadings significantly different from 0. The dashed line denotes our threshold of 2.6, corresponding to the critical value of Z at $p = 0.01$ (a value of 2 corresponds to $p = 0.05$). Important variables that were also significant and stable included the RMET, TASIT 1, TASIT 2 simple sarcasm, TASIT 2 paradoxical sarcasm, TASIT 3 sarcasm, processing speed, working memory, verbal learning, and visual learning. *EA LD1 contributions of connectivity variables with significant and stable* (**c**) *positive and* (**d**) *negative loadings*. **c** Positive loadings reflect increased connectivity in relation to better cognitive performance, and **d** negative loadings reflect reduced connectivity in relation to better cognitive performance. The regions of interest (ROIs) are organized according to the 12 Cole-Anticevic resting-state networks [60], and the subcortical regions [59]. Positive and negative connections (based on original mean sample connectivity values) are shown in red and blue, respectively (all significant and stable loadings were positive connections on average for EA LD1). *EA LD1 mean within- and between-network contributions of connectivity variables with significant and stable* (**e**) *positive and* (**f**) *negative loadings*. Contributions depicted represent the sum of contributions divided by the number of ROIs within each network and between each network for **e** positive loadings and **f** negative loadings. Positive and negative connections are shown in red and blue, respectively (all significant and stable loadings were positive connections on average for EA LD1).

confidence intervals of group means, and independent *t*-tests demonstrating significantly lower brain ($t(349.4) = -5.18$, $p < 0.001$, $pFDR < 0.001$; $d = -0.55$, 95% CI [−0.76, −0.33]) and behavior ($t(326.6) = -12.0$, $p < 0.001$, $pFDR < 0.001$; $d = -1.23$, 95% CI [−1.46, −1.00]) scores in the SSD group versus the control group. EA LD1 brain ($t(327.9) = -2.01$, $p = 0.045$, $pFDR = 0.091$; $d = -0.21$, 95% CI [−0.42, 0.01]) and behavior ($t(319.3) = 1.60$, $p = 0.110$, $pFDR = 0.110$; $d = 0.17$, 95% CI [−0.05, 0.38]) scores did not differ significantly based on sex. Across participants, lower brain and behavior scores were associated with increasing age ($r = -0.20$, $p < 0.001$, $pFDR < 0.001$; $r = -0.17$, $p = 0.002$, $pFDR = 0.002$) and higher mean FD ($r = -0.35$, $p < 0.001$, $pFDR < 0.001$; $r = -0.26$, $p < 0.001$, $pFDR < 0.001$) for EA LD1. In the SSD group, greater CPZE was associated with lower EA LD1 brain ($r = -0.22$, $p = 0.003$, $pFDR = 0.003$) and behavior ($r = -0.32$, $p < 0.001$, $pFDR < 0.001$) scores.

For EA LD2, brain and behavior scores were also significantly correlated in both SSD ($r = 0.299$, $p < 0.001$, $pFDR < 0.001$) and control ($r = 0.281$, $p < 0.001$, $pFDR < 0.001$) groups, but diagnostic groups were not distinguishable based on this LD (Fig. 3b). SSD and control groups showed overlapping 95% bootstrap confidence intervals, and did not differ significantly in brain ($t(340.8) = -1.8$, $p = 0.075$, $pFDR = 0.149$; $d = -0.19$, 95% CI [−0.40, 0.02]) or behavior ($t(350.0) = -1.41$, $p = 0.159$, $pFDR = 0.159$; $d = -0.15$, 95% CI [−0.36, 0.06]) scores. Though behavior scores did not differ significantly by sex ($t(297.9) = -1.79$, $p = 0.075$, $pFDR = 0.075$; $d = -0.19$, 95% CI [−0.41, 0.02]), female participants at birth had lower brain scores than males ($t(317.7) = -2.78$, $p = 0.006$, $pFDR = 0.011$; $d = -0.29$, 95% CI [−0.51, −0.08]) for EA LD2. Across participants, higher brain and behavior scores (reflecting worse performance) were associated with increasing age ($r = 0.30$, $p < 0.001$, $pFDR < 0.001$; $r = 0.24$, $p < 0.001$, $pFDR < 0.001$) and higher mean FD ($r = 0.32$, $p < 0.001$, $pFDR < 0.001$; $r = 0.15$, $p = 0.005$, $pFDR = 0.005$). EA LD2 brain ($r = 0.01$, $p = 0.901$, $pFDR = 0.955$) and behavior ($r = 0.00$, $p = 0.955$, $pFDR = 0.955$) scores were not significantly associated with CPZE in the SSD group.

Resting-State results

One LD from the resting-state PLSC survived the permutation test. Resting-state LD1 reflected a relationship between better performance across cognitive measures and increased connectivity across the somatomotor and visual networks, and decreased connectivity between the thalamus and these networks (Fig. 4). This LD explained 85.6% of brain-behavior covariance ($p = 0.001$), with a significant association between brain and behavior latent variable scores across groups ($r = 0.385$, $p < 0.001$). All social and non-social cognitive metrics loaded positively onto LD1, with all but TASIT 2 sincere showing significant and stable loadings (Fig. 4b). Of these, TASIT 1, TASIT 2 simple and paradoxical sarcasm, TASIT 3 sarcasm, processing speed, verbal and visual learning, and reasoning and problem solving were important contributors to resting-state LD1 (Fig. 4a). Higher scores on these cognitive metrics were associated with increased positive connectivity within the somatomotor, primary and secondary visual, auditory, and posterior-multimodal networks, and between the somatomotor and both visual networks, secondary visual-dorsal attention networks, and language-auditory networks, among others (positive loadings; Figs. 4c and 4e). The same behavioral patterns were also associated with decreased positive connectivity between the ventral and dorsal anterior thalamus and the somatomotor, primary visual, auditory, and language networks, as well as decreased negative connectivity between these subcortical regions and the secondary visual network (negative loadings; Figs. 4d and 4f). A second LD was identified that showed a similar behavioral pattern to EA LD2, including generally poorer social cognition and enhanced non-social cognition in relation to connectivity patterns, but it was non-significant and explained only 2.5% of the brain-behavior covariance ($p = 0.48$).

Resting-State post-hoc analyses

Brain and behavior latent variable scores for resting-state LD1 were significantly correlated in the SSD ($r = 0.312$, $p < 0.001$, $pFDR < 0.001$) but not the control group ($r = 0.0152$, $p = 0.85$, $pFDR = 0.85$). SSD and control groups also differed significantly in resting-state LD1 (Fig. 5a) according to non-overlapping group mean 95% bootstrap confidence intervals, and *t*-tests showing significantly lower brain ($t(301.5) = -9.42$, $p < 0.001$, $pFDR < 0.001$; $d = -1.03$, 95% CI [−1.25, −0.81]) and behavior ($t(328.13) = -12.2$, $p < 0.001$, $pFDR < 0.001$; $d = -1.24$, 95% CI [−1.47, −1.01]) scores in the SSD group compared to controls. There were no significant sex-based differences in resting-state LD1 brain ($t(273.6) = -0.262$, $p = 0.79$, $pFDR = 0.79$; $d = -0.03$, 95% CI [−0.24, 0.19]) or behavior ($t(317.15) = 1.57$, $p = 0.12$, $pFDR = 0.23$; $d = 0.17$, 95% CI [−0.05, 0.38]) scores. Across participants, brain scores were positively correlated with resting-state mean FD ($r = 0.14$, $p = 0.0089$, $pFDR = 0.013$) but not age ($r = 0.02$, $p = 0.71$, $pFDR = 0.71$), whereas behavior scores were significantly negatively associated with age ($r = -0.16$, $p = 0.0032$, $pFDR = 0.018$) but not mean FD ($r = -0.05$, $p = 0.34$, $pFDR = 0.45$). CPZEs were significantly negatively correlated with both brain ($r = -0.21$, $p = 0.005$, $pFDR = 0.005$) and behavior ($r = -0.31$, $p < 0.001$, $pFDR < 0.001$) scores in the SSD group.

Robustness and stability analyses

Both the 10-fold and 4-fold cross-validation analyses demonstrated significant reliability via high correlations between

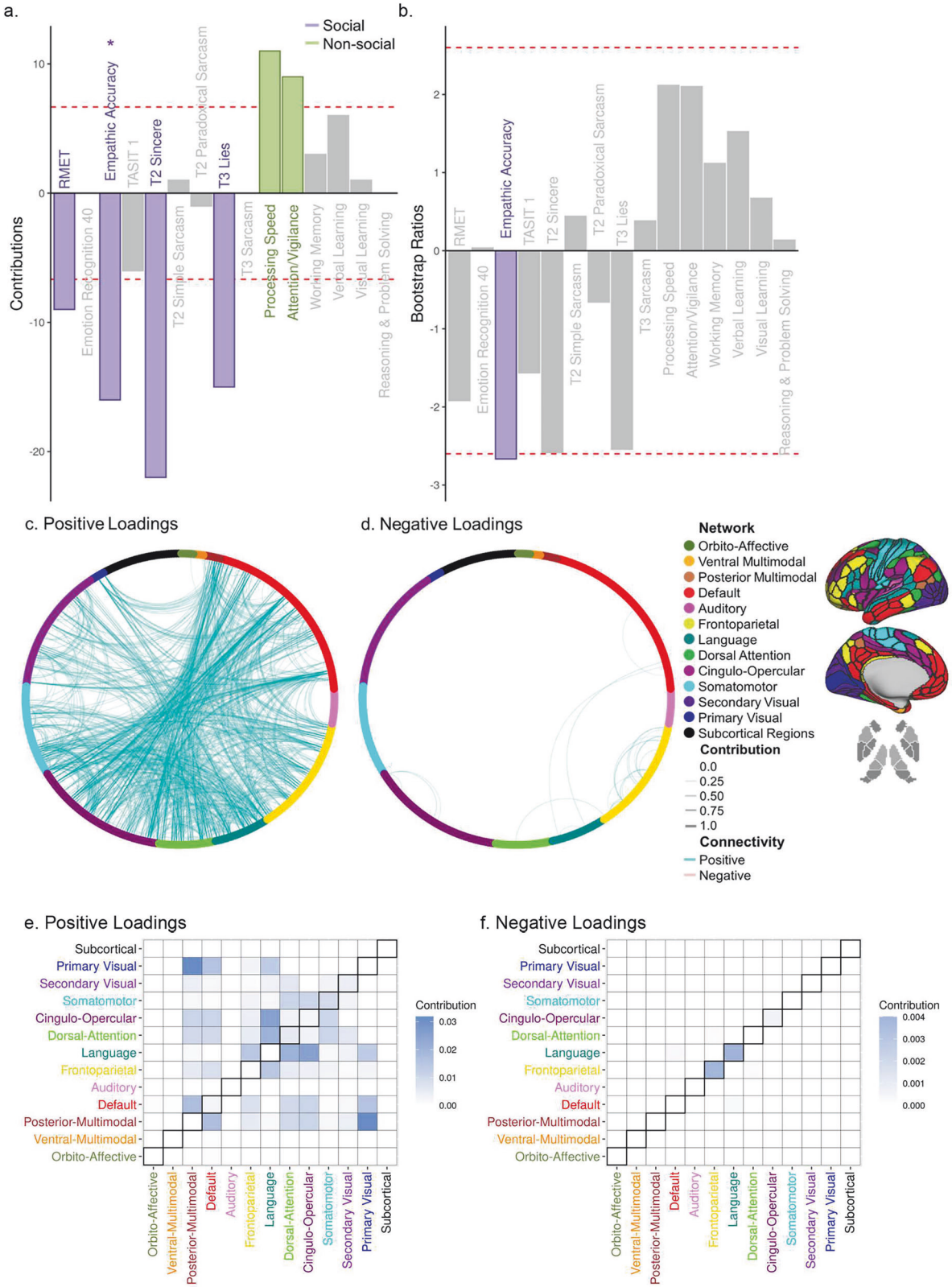

originally observed and predicted brain and behavior latent variable scores (all $r > 0.90$, $p < 0.001$), and between the observed and estimated brain and behavior loadings (all $r >= 0.90$) for both the EA and resting-state PLSC models (see Supplementary Material). The proportion of variance explained by EA LD1, EA LD2, and resting-state LD1 was also highly similar across folds for both 10-fold and 4-fold analyses (see Supplementary Material). PLSC results using only one EA run confirmed EA model stability, with correlations of $r > 0.90$ between brain and behavior latent variables across both significant LDs (see Supplementary Material).

Fig. 2 EA Latent Dimension (LD) 2. *EA LD2* (**a**) *behavioral effect sizes* (**b**) *and loading stability*. **a** Contributions of behavioral variables for EA LD2. Contributions are calculated as the squared loadings and quantify the amount of variance contributed to the LD by each variable, indicating the effect size. The direction of the contributions reflects the loading direction. Variables with contributions that exceed the dashed line, which represents the average contribution, can be considered important [110]. Asterisks indicate those that were significant and stable according to bootstrap ratios. **b** Bootstrap ratios of behavioral loadings for EA LD2. A bootstrap procedure was used to identify variables with loadings significantly different from 0. The dashed line denotes our threshold of 2.6, corresponding to the critical value of Z at $p = 0.01$ (a value of 2 corresponds to $p = 0.05$). EA was the only important contributing variable identified as significant and stable. *EA LD2 contributions of connectivity variables with significant and stable* (**c**) *positive and* (**d**) *negative loadings*. **c** Positive loadings reflect increased connectivity and **d** negative loadings reflect reduced connectivity in relation to decreased social cognitive and increased non-social cognitive performance. The regions of interest (ROIs) are organized according to the 12 Cole-Anticevic resting-state networks [60], and the subcortical regions [59]. Positive and negative connections (based on original mean sample connectivity values) are shown in red and blue, respectively (all significant and stable loadings were positive connections on average for EA LD2). *EA LD2 mean within- and between-network contributions of connectivity variables with significant and stable* (**e**) *positive and* (**f**) *negative loadings*. Contributions depicted represent the sum of contributions divided by the number of ROIs within each network and between each network for **e** positive loadings and **f** negative loadings. Positive and negative connections are shown in red and blue, respectively (all significant and stable loadings were positive connections on average for EA LD2).

PLSC results for EA and resting-state after regressing out age, sex, and mean FD also showed very similar patterns to the observed results, with correlations of $r > 0.80$ between brain and behavior latent variables across analyses for all significant LDs (see Supplementary Material).

DISCUSSION

The present study used multivariate analyses to identify LDs capturing relationships between social and non-social cognitive performance and functional connectivity during social task-based and resting-state fMRI, across a large sample of individuals with SSDs and healthy controls. Though functional connectivity patterns during social processing and at rest were both associated with global cognition, our results suggest that social task-based connectivity can delineate patterns and explain more of the variance related to particular social cognitive functions than resting-state connectivity. The first significant LD for both EA and resting-state analyses distinguished between SSD and control groups, and reflected a relationship between better overall cognitive performance and some overlapping but largely divergent functional connectivity patterns. Networks implicated in processing dynamic multimodal and social stimuli preferentially contributed during social processing, whereas somatomotor, visual, and subcortical connectivity contributed most at rest. A second LD was also significant for the EA task analysis, which did not differentiate diagnostic groups, revealing an association between worse EA performance and increased connectivity between more socially relevant networks.

EA LD1 demonstrated a relationship between better cognition and increased connectivity within and between networks involved in processing dynamic multimodal stimuli (language, auditory, somatomotor, and secondary visual networks) and socioemotional processing, including the cingulo-opercular, frontoparietal, and default networks that overlap with the simulation and mentalizing networks [19]. This pattern likely reflects appropriate processing and integration of the EA stimuli, including language, salient sensory, and emotional information [76], in relation to better overall cognitive performance. Despite distinguishing between diagnostic groups, the significant correlation between brain and behavior scores in both groups supports a continuous relationship across participants, similar to the dimensional multivariate relationship previously identified between white matter circuitry and cognition (social and non-social) in the SPINS sample [77].

EA LD2 captured a relationship between worse EA performance and increased connectivity between multiple socially relevant networks, including the language, cingulo-opercular, default, and frontoparietal networks, as well as dorsal attention and primary visual networks, which may reflect social more than sensory processing of the video stimuli. LD2 involved more between-network connectivity compared to more within-network connectivity observed in LD1, and did not differentiate between diagnostic groups. These findings broadly align with previous work from our group identifying greater positive functional connectivity and reduced segregation between social cognitive networks during the EA task [41], and inefficient network activation patterns during an emotional imitation task [78], in worse social cognitive performers across SSDs and healthy controls. This increased connectivity between socially relevant networks may indicate compensatory hyperconnectivity or integration issues across these different networks in poorer social cognitive performers [79, 80]. Such a pattern could represent inefficient network activation and broader recruitment of regions beyond those most relevant to the task, arising from increased neural effort to achieve the same social cognitive process, or engagement of qualitatively different processes [41, 78]. Aberrant connectivity among the default, frontoparietal, and cingulo-opercular (or salience) networks has also been linked to depressive symptoms in schizophrenia [70, 81], which have been associated with poorer social functioning [82]; however, relationships between cognitive performance and depressive symptoms in SSDs are complex and additional work is needed to clarify how these processes interact, especially in the context of task-based fMRI [83].

Interestingly, social cognitive metrics, and lower-level measures in particular, were generally negatively associated with the corresponding increased positive connectivity, whereas neurocognitive measures were positively associated for EA LD2. These findings align with evidence suggesting that social and non-social cognition are at least partially dissociable constructs [6, 84, 85], despite shared variance, which may differentially benefit from network segregation for specialized social processing versus integration for more cognitively demanding tasks [19, 86]. However, only EA scores exhibited significant and stable loadings onto this LD, rather than robustly delineating lower- and higher-level social cognitive and non-social cognitive constructs. These results emphasize the utility of task-based paradigms to better understand particular cognitive abilities, but could suggest that a more hypothesis- versus data-driven approach may better distinguish between connectivity profiles associated with correlated cognitive domains.

Resting-state LD1 captured a relationship between better general cognitive performance and increased somatomotor and visual within- and between-network connectivity, as well as decreased thalamo-cortical connectivity, which appeared to be driven more by the SSD group. Prior resting-state fMRI findings in SSDs versus healthy controls have highlighted somatomotor and visual network dysconnectivity [87], including using functional connectivity gradients in the SPINS sample [88], as well as thalamic-somatomotor hyperconnectivity [89–92]. Lower-order

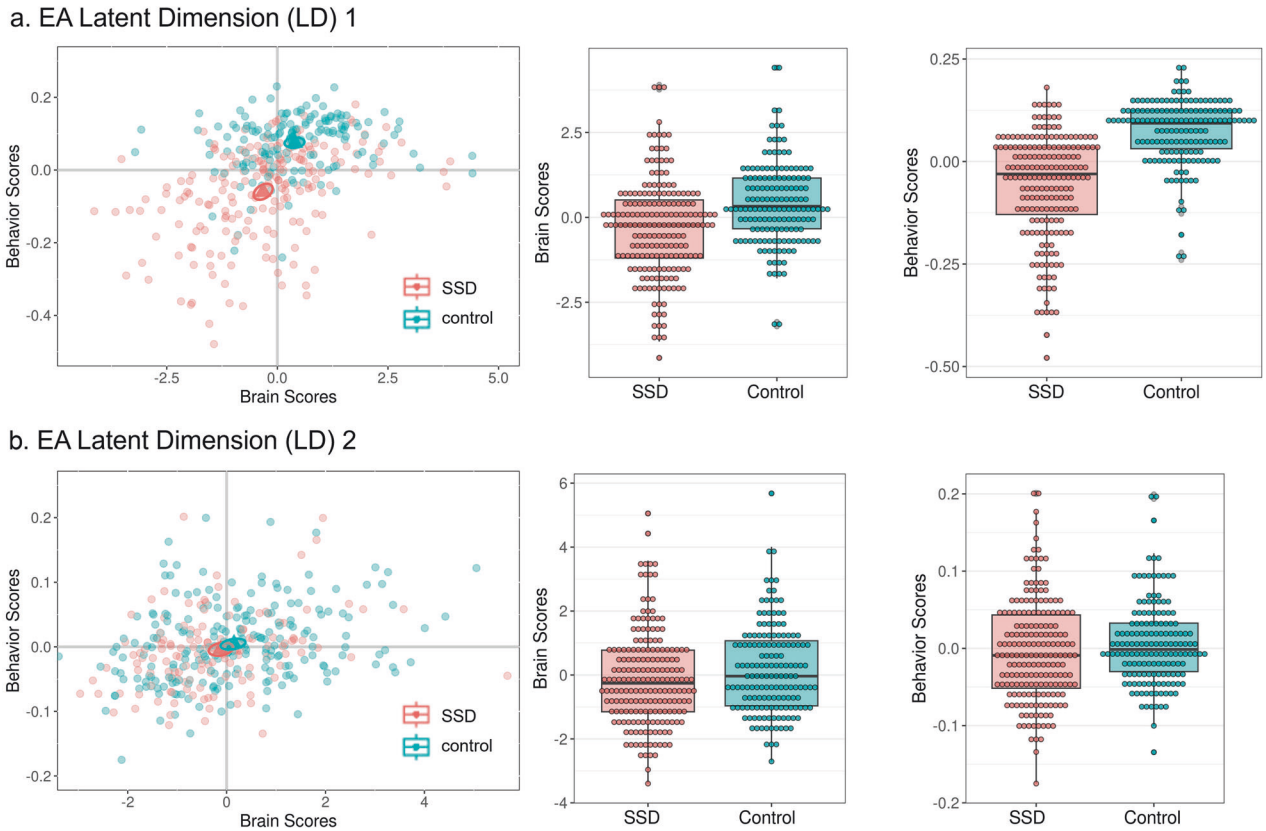

Fig. 3 EA Behavior and Brain Scores by Diagnostic Group. EA (**a**) Latent Dimension (LD) 1 and (**b**) LD2 Behavior and Brain Scores by Diagnostic Group. Scatterplots depict the association between behavior and brain connectivity latent variable scores, with individual participant data points colored by diagnostic group. Triangles represent group means with ellipsoids showing 95% bootstrap confidence intervals, where non-overlapping confidence intervals indicate a significant difference between groups. Boxplots depict brain (left) and behavior (right) latent variable scores by diagnostic group.

sensory impairments are also common in SSDs and may broadly influence downstream cognitive functions [93, 94]. A recent transdiagnostic PLS analysis, including schizophrenia, also similarly identified a LD characterized by broad non-social cognition and resting-state somatomotor and visual network connectivity, though they were negatively related [28]. Notably, our analyses did not delineate significant relationships specific to social cognition for the resting-state data, and though some default network connectivity contributed to resting-state LD1, it did not feature prominently. A review of studies examining non-social cognition and resting-state functional connectivity in schizophrenia similarly provided evidence for shared neural correlates underlying a generalized cognitive deficit, including aberrant subcortical-cortical, as well as default and cingulo-opercular connectivity [27]. More broadly, whole-brain resting-state functional connectivity patterns have been associated with positive versus negative traits [95] and used to predict fluid intelligence [96], personality dimensions [97], and brain maturity/age [98, 99] in large typically developing and/or community samples. Overall, the resting-state LD appeared to involve network dysfunction often implicated in SSDs and other psychiatric disorders, aligning with this LD being driven by the SSD group, but did not distinguish between aspects of cognition, suggesting that it is generally informative but lacks cognitive specificity.

Across EA and rest, LD1 reflected associations between global cognition and functional connectivity patterns across several networks, with more secondary visual, somatomotor, dorsal attention, and thalamic connectivity contributing at rest and EA featuring more association networks. This suggests that general social and non-social cognition are represented by widespread brain connectivity, aligning with literature demonstrating associations between connectivity across the whole brain and overall cognitive ability (the 'g' factor) [100, 101]. Interestingly, though both EA and resting-state LD1 distinguished between diagnostic groups, brain and behavior scores were not significantly correlated for controls during rest. Thus, the EA task appears to reveal dimensional functional connectivity-cognition relationships across SSDs and controls, as well as case-control differences, whereas the unconstrained nature of resting-state data may emphasize broader diagnostic differences [38]. Further, the EA task PLSC analysis identified two significant LDs, with the second reflecting EA in particular, whereas the resting-state PLSC identified only one. Naturalistic and task-based fMRI have been found to increase sensitivity to behavioral differences and allow for greater interpretability and experimental control [32–34]. Some work has also suggested that resting-state connectivity may be less congruent with task-evoked activation during social perception in people with schizophrenia than healthy controls [102]. Taken together, these results highlight the importance of selecting imaging metrics and paradigms tailored to your research question, where task-based imaging may be preferable for understanding specific cognitive domains and behavioral metrics [103].

Though post-hoc analyses demonstrated relationships between brain and behavior scores across the identified LDs and both age and motion during scanning, it is reassuring that we see similar patterns emerge when we regress out the effects of age, sex, and mean FD prior to PLSC analyses. Regarding other potential limitations, the significant association between EA and resting-state LD1 brain and behavior scores and CPZEs in the SSD group suggests that greater antipsychotic medication load is associated

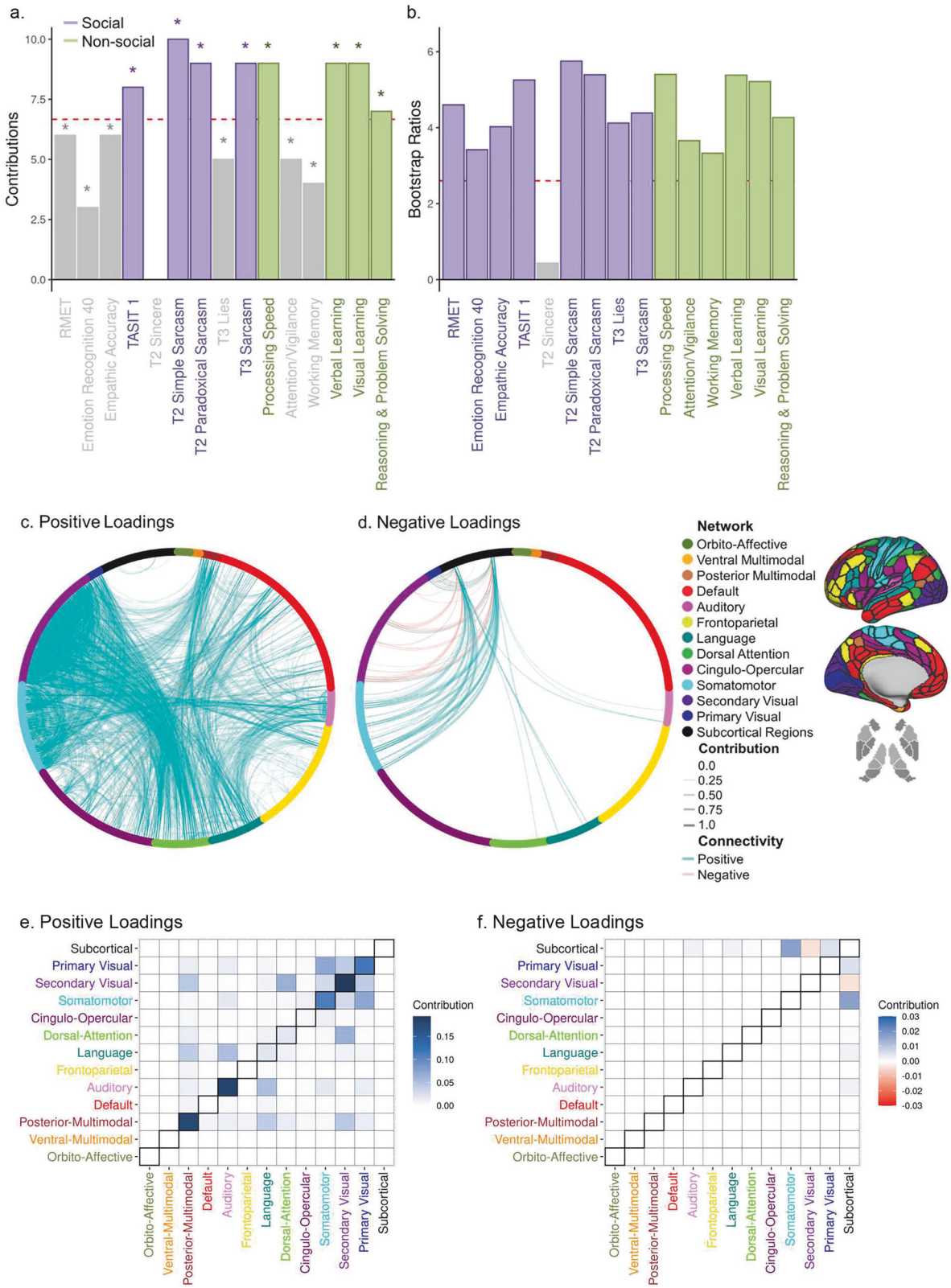

with worse general cognition, aligning with some evidence suggesting that antipsychotic medication negatively impacts cognition [104], though results are mixed and there may be confounding factors [105, 106]. Additional work examining the relationship between antipsychotic medication and both cognition and functional connectivity is needed. We examined cortical and subcortical connectivity in the present analyses given the availability and integration of corresponding atlas parcellations, but the role of the cerebellum in social cognition has recently been highlighted [107, 108] and future work should

Fig. 4 Resting-State Latent Dimension (LD) 1. *Resting-state LD1* (**a**) *behavioral effect sizes* (**b**) *and loading stability*. **a** Contributions of behavioral variables for resting-state LD1. Contributions are calculated as the squared loadings and quantify the amount of variance contributed to the LD by each variable, indicating the effect size. The direction of the contributions reflects the loading direction. Variables with contributions that exceed the dashed line, which represents the average contribution, can be considered important [110]. Asterisks indicate those that were significant and stable according to bootstrap ratios. **b** Bootstrap ratios of behavioral loadings for resting-state LD1. A bootstrap procedure was used to identify variables with loadings significantly different from 0. The dashed line denotes our threshold of 2.6, corresponding to the critical value of Z at $p = 0.01$ (a value of 2 corresponds to $p = 0.05$). Important variables that were also significant and stable included TASIT 1, TASIT 2 simple sarcasm, TASIT 2 paradoxical sarcasm, TASIT 3 sarcasm, processing speed, verbal learning, visual learning, and reasoning and problem solving. *Resting-state LD1 contributions of connectivity variables with significant and stable* (**c**) *positive and* (**d**) *negative loadings*. **c** Positive loadings reflect increased connectivity in relation to better cognitive performance, and **d** negative loadings reflect reduced connectivity in relation to better cognitive performance. The regions of interest (ROIs) are organized according to the 12 Cole-Anticevic resting-state networks [60], and the subcortical regions [59]. Positive and negative connections (based on original mean sample connectivity values) are shown in red and blue, respectively. *Resting-state LD1 mean within- and between-network contributions of connectivity variables with significant and stable* (**e**) *positive and* (**f**) *negative loadings*. Contributions depicted represent the sum of contributions divided by the number of ROIs within each network and between each network for **e** positive loadings and **f** negative loadings. Positive and negative connections are shown in red and blue, respectively.

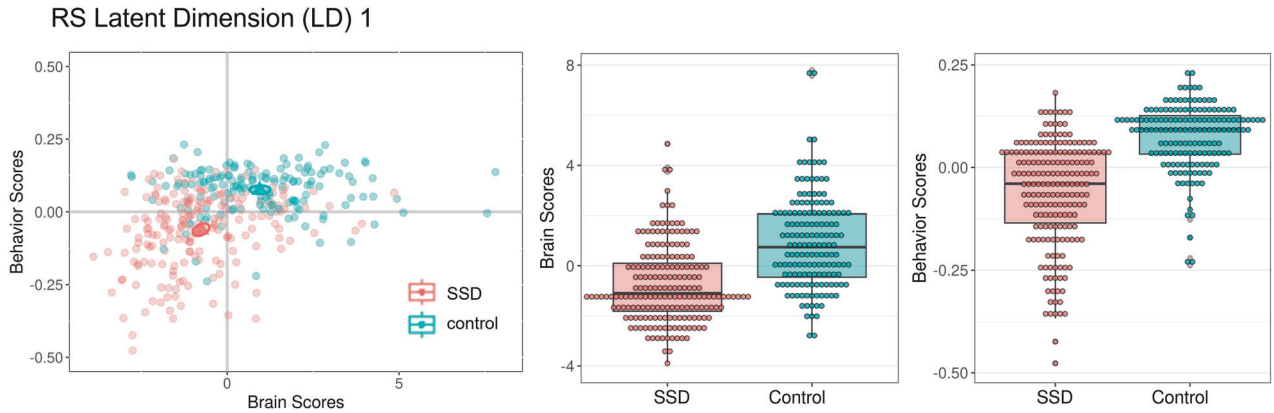

Fig. 5 Resting-State Behavior and Brain Scores by Diagnostic Group. Resting-State Latent Dimension (LD) 1 Behavior and Brain Scores by Diagnostic Group. The scatterplot depicts the association between behavior and brain connectivity latent variable scores, with individual participant data points colored by diagnostic group. Triangles represent group means with ellipsoids showing 95% bootstrap confidence intervals, where non-overlapping confidence intervals indicate a significant difference between groups. Boxplots depict brain (left) and behavior (right) latent variable scores by diagnostic group.

incorporate this region [109]. Our PLSC results are also inherently constrained by the input variables included in these analyses and the inclusion of different variables or parcellations may have produced different results. While reproducibility and reliability remain challenges in brain-behavior research, the present study mitigates these concerns through using validated performance-based cognitive measures, models with and without covariate adjustment, and both 10-fold and 4-fold cross-validation analyses to support the robustness of our findings. It should also be noted that our resting-state scan duration was 7 min based on accepted practices at the time of collection, though our EA model stability analyses suggest that the EA findings are highly consistent and differences between the EA and resting-state results are not due to scan duration or the amount of fMRI data acquired. Nonetheless, external replication in independent samples will be critical to substantiate our findings and confirm generalizability, and longitudinal investigations are needed to assess scan-rescan reliability and understand how these relationships may change over time.

Our results suggest that functional connectivity patterns during social processing and at rest are associated with both social and non-social cognitive performance across people with SSDs and healthy controls. Some overlapping, but largely divergent, connectivity patterns appear to covary with better cognitive performance during social processing compared to rest. In particular, increased connectivity in more socially relevant networks during the EA task was negatively associated with lower-level social cognitive performance. Dimensional relationships across SSDs and healthy controls were also identified using the EA task, whereas the resting-state findings appeared to be driven more by the SSD group. These results provide support for the value of task-based fMRI to identify dimensional functional connectivity patterns associated with particular cognitive functions that may not be disorder-specific.

Supplementary information is available at Molecular Psychiatry's website.

REFERENCES

1. Couture SM, Penn DL, Roberts DL. The functional significance of social cognition in schizophrenia: a review. Schizophr Bull. 2006;32:S44–63.
2. Green MF, Kern RS, Heaton RK. Longitudinal studies of cognition and functional outcome in schizophrenia: implications for MATRICS. Schizophr Res. 2004;72:41–51.
3. Savla GN, Vella L, Armstrong CC, Penn DL, Twamley EW. Deficits in domains of social cognition in schizophrenia: a meta-analysis of the empirical evidence. Schizophr Bull. 2013;39:979–92.
4. Kern RS, Gold JM, Dickinson D, Green MF, Nuechterlein KH, Baade LE, et al. The MCCB impairment profile for schizophrenia outpatients: results from the MATRICS psychometric and standardization study. Schizophr Res. 2011;126:124–31.
5. Green MF, Horan WP, Lee J. Nonsocial and social cognition in schizophrenia: current evidence and future directions. World Psychiatry. 2019;18:146–61.
6. Oliver LD, Haltigan JD, Gold JM, Foussias G, DeRosse P, Buchanan RW, et al. Lower- and higher-level social cognitive factors across individuals with schizophrenia spectrum disorders and healthy controls: relationship with neurocognition and functional outcome. Schizophrenia Bulletin. 2019;45:629–38.

7. Thibaudeau É, Achim AM, Parent C, Turcotte M, Cellard C. A meta-analysis of the associations between theory of mind and neurocognition in schizophrenia. Schizophr Res. 2020;216:118–28.
8. Fett A-KJ, Viechtbauer W, Dominguez M-G, Penn DL, van Os J, Krabbendam L. The relationship between neurocognition and social cognition with functional outcomes in schizophrenia: a meta-analysis. Neurosci Biobehav Rev. 2011;35:573–88.
9. Halverson TF, Orleans-Pobee M, Merritt C, Sheeran P, Fett A-K, Penn DL. Pathways to functional outcomes in schizophrenia spectrum disorders: Meta-analysis of social cognitive and neurocognitive predictors. Neurosci Biobehav Rev. 2019;105:212–9.
10. Jáni M, Kašpárek T. Emotion recognition and theory of mind in schizophrenia: a meta-analysis of neuroimaging studies. World J Biol Psychiatry. 2018;19:S86–S96.
11. Taylor SF, Kang J, Brege IS, Tso IF, Hosanagar A, Johnson TD. Meta-analysis of functional neuroimaging studies of emotion perception and experience in schizophrenia. Biol Psychiatry. 2012;71:136–45.
12. Kronbichler L, Tschernegg M, Martin AI, Schurz M, Kronbichler M. Abnormal brain activation during theory of mind tasks in schizophrenia: a meta-analysis. Schizophr Bull. 2017;43:1240–50.
13. Mukherjee P, Whalley HC, McKirdy JW, Sprengelmeyer R, Young AW, McIntosh AM, et al. Altered amygdala connectivity within the social brain in schizophrenia. Schizophr Bull. 2014;40:152–60.
14. Mier D, Eisenacher S, Rausch F, Englisch S, Gerchen MF, Zamoscik V, et al. Aberrant activity and connectivity of the posterior superior temporal sulcus during social cognition in schizophrenia. Eur Arch Psychiatry Clin Neurosci. 2017;267:597–610.
15. Molenberghs P, Cunnington R, Mattingley JB. Brain regions with mirror properties: a meta-analysis of 125 human fMRI studies. Neuroscience & Biobehavioral Reviews. 2012;36:341–9.
16. Carr L, Iacoboni M, Dubeau M-C, Mazziotta JC, Lenzi GL. Neural mechanisms of empathy in humans: a relay from neural systems for imitation to limbic areas. Proc Natl Acad Sci USA. 2003;100:5497–502.
17. Carrington SJ, Bailey AJ. Are there theory of mind regions in the brain? a review of the neuroimaging literature. Hum Brain Mapp. 2009;30:2313–35.
18. Schurz M, Radua J, Aichhorn M, Richlan F, Perner J. Fractionating theory of mind: a meta-analysis of functional brain imaging studies. Neurosci Biobehav Rev. 2014;42:9–34.
19. Schurz M, Maliske L, Kanske P. Cross-network interactions in social cognition: a review of findings on task related brain activation and connectivity. Cortex. 2020;130:142–57.
20. Doruyter A, Groenewold NA, Dupont P, Stein DJ, Warwick JM Resting-state fMRI and social cognition: an opportunity to connect. Hum Psychopharmacol. 2017;32.
21. Schilbach L, Bzdok D, Timmermans B, Fox PT, Laird AR, Vogeley K, et al. Introspective minds: using ALE meta-analyses to study commonalities in the neural correlates of emotional processing, social & unconstrained cognition. PLoS One. 2012;7:e30920.
22. Amft M, Bzdok D, Laird AR, Fox PT, Schilbach L, Eickhoff SB. Definition and characterization of an extended social-affective default network. Brain Struct Funct. 2015;220:1031–49.
23. Abram SV, Wisner KM, Fox JM, Barch DM, Wang L, Csernansky JG, et al. Fronto-temporal connectivity predicts cognitive empathy deficits and experiential negative symptoms in schizophrenia. Hum Brain Mapp. 2017;38:1111–24.
24. Mothersill O, Tangney N, Morris DW, McCarthy H, Frodl T, Gill M, et al. Further evidence of alerted default network connectivity and association with theory of mind ability in schizophrenia. Schizophr Res. 2017;184:52–58.
25. Zemánková P, Lošák J, Czekóová K, Lungu O, Jáni M, Kašpárek T, et al. Theory of mind skills are related to resting-state frontolimbic connectivity in schizophrenia. Brain Connect. 2018;8:350–61.
26. Choe E, Lee TY, Kim M, Hur J-W, Yoon YB, Cho K-IK, et al. Aberrant within- and between-network connectivity of the mirror neuron system network and the mentalizing network in first episode psychosis. Schizophr Res. 2018;199:243–9.
27. Sheffield JM, Barch DM. Cognition and resting-state functional connectivity in schizophrenia. Neurosci Biobehav Rev. 2016;61:108–20.
28. Kebets V, Holmes AJ, Orban C, Tang S, Li J, Sun N, et al. Somatosensory-Motor dysconnectivity spans multiple transdiagnostic dimensions of psychopathology. Biol Psychiatry. 2019;86:779–91.
29. Baker JT, Dillon DG, Patrick LM, Roffman JL, Brady RO Jr, et al. Functional connectomics of affective and psychotic pathology. Proc Natl Acad Sci USA. 2019;116:9050–9.
30. Ma Q, Tang Y, Wang F, Liao X, Jiang X, Wei S, et al. transdiagnostic dysfunctions in brain modules across patients with schizophrenia, bipolar disorder, and major depressive disorder: a connectome-based study. Schizophr Bull. 2020;46:699–712.
31. Viviano JD, Buchanan RW, Calarco N, Gold JM, Foussias G, Bhagwat N, et al. Resting-State connectivity biomarkers of cognitive performance and social function in individuals with schizophrenia spectrum disorder and healthy control subjects. Biol Psychiatry. 2018;84:665–74.
32. Finn ES. Is it time to put rest to rest? Trends Cogn Sci. 2021;25:1021–32.
33. Greene AS, Gao S, Scheinost D, Constable RT. Task-induced brain state manipulation improves prediction of individual traits. Nat Commun. 2018;9:2807.
34. Finn ES, Bandettini PA. Movie-watching outperforms rest for functional connectivity-based prediction of behavior. Neuroimage. 2021;235:117963.
35. Patel GH, Arkin SC, Ruiz-Betancourt DR, Plaza FI, Mirza SA, Vieira DJ, et al. Failure to engage the temporoparietal junction/posterior superior temporal sulcus predicts impaired naturalistic social cognition in schizophrenia. Brain. 2021;144:1898–910.
36. Martin AK, Dzafic I, Robinson GA, Reutens D, Mowry B. Mentalizing in schizophrenia: a multivariate functional MRI study. Neuropsychologia. 2016;93:158–66.
37. Bitsch F, Berger P, Nagels A, Falkenberg I, Straube B. Characterizing the theory of mind network in schizophrenia reveals a sparser network structure. Schizophr Res. 2021;228:581–9.
38. Secara MT, Oliver LD, Gallucci J, Dickie EW, Foussias G, Gold J, et al. Heterogeneity in functional connectivity: dimensional predictors of individual variability during rest and task fMRI in psychosis. Prog Neuropsychopharmacol Biol Psychiatry 2024;132:110991.
39. Kern RS, Penn DL, Lee J, Horan WP, Reise SP, Ochsner KN, et al. Adapting social neuroscience measures for schizophrenia clinical trials, Part 2: trolling the depths of psychometric properties. Schizophr Bull. 2013;39:1201–10.
40. Olbert CM, Penn DL, Kern RS, Lee J, Horan WP, Reise SP, et al. Adapting social neuroscience measures for schizophrenia clinical trials, part 3: fathoming external validity. Schizophr Bull. 2013;39:1211–8.
41. Oliver LD, Hawco C, Homan P, Lee J, Green MF, Gold JM, et al. Social cognitive networks and social cognitive performance across individuals with schizophrenia spectrum disorders and healthy control participants. Biological Psychiatry: Cognitive Neuroscience and Neuroimaging. 2020;6:1202–14.
42. Leucht S, Samara M, Heres S, Davis JM. Dose equivalents for antipsychotic drugs: the DDD method. Schizophr Bull. 2016;42:S90–4.
43. Gardner DM, Murphy AL, O'Donnell H, Centorrino F, Baldessarini RJ. International consensus study of antipsychotic dosing. Am J Psychiatry. 2010;167:686–93.
44. Pinkham AE, Penn DL, Green MF, Buck B, Healey K, Harvey PD. The social cognition psychometric evaluation study: results of the expert survey and RAND panel. Schizophr Bull. 2014;40:813–23.
45. Kohler CG, Bilker W, Hagendoorn M, Gur RE, Gur RC. Emotion recognition deficit in schizophrenia: association with symptomatology and cognition. Biol Psychiatry. 2000;48:127–36.
46. Baron-Cohen S, Wheelwright S, Hill J, Raste Y, Plumb I. The "Reading the Mind in the Eyes" test revised version: a study with normal adults, and adults with asperger syndrome or high-functioning autism. J Child Psychol Psychiatry. 2001;42:241–51.
47. McDonald S, Flanagan S, Rollins J, Kinch J. TASIT: A new clinical tool for assessing social perception after traumatic brain injury. J Head Trauma Rehabil. 2003;18:219–38.
48. Nuechterlein KH, Green MF, Kern RS, Baade LE, Barch DM, Cohen JD, et al. The MATRICS consensus cognitive battery, part 1: test selection, reliability, and validity. Am J Psychiatry. 2008;165:203–13.
49. Harvey P-O, Zaki J, Lee J, Ochsner K, Green MF. Neural substrates of empathic accuracy in people with schizophrenia. Schizophr Bull. 2013;39:617–28.
50. Zaki J, Weber J, Bolger N, Ochsner K. The neural bases of empathic accuracy. Proc Natl Acad Sci USA. 2009;106:11382–7.
51. Kral TRA, Solis E, Mumford JA, Schuyler BS, Flook L, Rifken K, et al. Neural correlates of empathic accuracy in adolescence. Soc Cogn Affect Neurosci. 2017;12:1701–10.
52. Esteban O, Markiewicz CJ, Blair RW, Moodie CA, Isik AI, Erramuzpe A, et al. fMRIPrep: a robust preprocessing pipeline for functional MRI. Nat Methods. 2019;16:111–6.
53. Avants BB, Epstein CL, Grossman M, Gee JC. Symmetric diffeomorphic image registration with cross-correlation: evaluating automated labeling of elderly and neurodegenerative brain. Med Image Anal. 2008;12:26–41.
54. Zhang Y, Brady M, Smith S. Segmentation of brain MR images through a hidden Markov random field model and the expectation-maximization algorithm. IEEE Trans Med Imaging. 2001;20:45–57.
55. Dale AM, Fischl B, Sereno MI. Cortical surface-based analysis. I. Segmentation and surface reconstruction. Neuroimage. 1999;9:179–94.
56. Cox RW, Hyde JS. Software tools for analysis and visualization of fMRI data. NMR Biomed. 1997;10:171–8.

57. Jenkinson M, Bannister P, Brady M, Smith S. Improved optimization for the robust and accurate linear registration and motion correction of brain images. Neuroimage. 2002;17:825–41.
58. Treiber JM, White NS, Steed TC, Bartsch H, Holland D, Farid N, et al. Characterization and correction of geometric distortions in 814 diffusion weighted images. PLoS One. 2016;11:e0152472.
59. Dickie EW, Anticevic A, Smith DE, Coalson TS, Manogaran M, Calarco N, et al. Ciftify: a framework for surface-based analysis of legacy MR acquisitions. Neuroimage. 2019;197:818–26.
60. Gorgolewski K, Burns CD, Madison C, Clark D, Halchenko YO, Waskom ML, et al. Nipype: a flexible, lightweight and extensible neuroimaging data processing framework in python. Front Neuroinform. 2011;5:13.
61. Al-Aidroos N, Said CP, Turk-Browne NB. Top-down attention switches coupling between low-level and high-level areas of human visual cortex. Proc Natl Acad Sci USA. 2012;109:14675–80.
62. Norman-Haignere SV, McCarthy G, Chun MM, Turk-Browne NB. Category-selective background connectivity in ventral visual cortex. Cereb Cortex. 2012;22:391–402.
63. Glasser MF, Coalson TS, Robinson EC, Hacker CD, Harwell J, Yacoub E, et al. A multi-modal parcellation of human cerebral cortex. Nature. 2016;536:171–8.
64. Tian Y, Margulies DS, Breakspear M, Zalesky A. Topographic organization of the human subcortex unveiled with functional connectivity gradients. Nat Neurosci. 2020;23:1421–32.
65. Ji JL, Spronk M, Kulkarni K, Repovš G, Anticevic A, Cole MW. Mapping the human brain's cortical-subcortical functional network organization. Neuroimage. 2019;185:35–57.
66. Fortin J-P, Cullen N, Sheline YI, Taylor WD, Aselcioglu I, Cook PA, et al. Harmonization of cortical thickness measurements across scanners and sites. Neuroimage. 2018;167:104–20.
67. RStudio T RStudio: integrated development for R. Boston, MA: RStudio. Inc[Google Scholar].
68. Beaton D, Chin Fatt CR, Abdi H. An ExPosition of multivariate analysis with the singular value decomposition in R. Comput Stat Data Anal. 2014;72:176–89.
69. McIntosh AR, Lobaugh NJ. Partial least squares analysis of neuroimaging data: applications and advances. Neuroimage. 2004;23:S250–63.
70. Gallucci J, Yu J-C, Oliver LD, Nakua H, Zhukovsky P, Dickie EW, et al. Neural circuitry and therapeutic targeting of depressive symptoms in schizophrenia spectrum disorders. Am J Psychiatry. 2024;181:910–9.
71. Xia CH, Ma Z, Ciric R, Gu S, Betzel RF, Kaczkurkin AN, et al. Linked dimensions of psychopathology and connectivity in functional brain networks. Nat Commun. 2018;9:3003.
72. Sun L, Ji S, Yu S, Ye J On the equivalence between canonical correlation analysis and orthonormalized partial least squares. Proceedings of the 21st International Joint Conference on Artificial Intelligence, 2009. p. 1230-5.
73. Krishnan A, Williams LJ, McIntosh AR, Abdi H. Partial Least squares (PLS) methods for neuroimaging: a tutorial and review. Neuroimage. 2011;56:455–75.
74. Takane Y, Hwang H. Generalized constrained canonical correlation analysis. Multivariate Behav Res. 2002;37:163–95.
75. Winkler AM, Renaud O, Smith SM, Nichols TE. Permutation inference for canonical correlation analysis. Neuroimage. 2020;220:117065.
76. Uddin LQ, Yeo BTT, Spreng RN. Towards a universal taxonomy of macro-scale functional human brain networks. Brain Topogr. 2019;32:926–42.
77. Calarco N, Oliver LD, Joseph M, Hawco C, Dickie EW, DeRosse P, et al. Multivariate associations among white matter, neurocognition, and social cognition across individuals with schizophrenia spectrum disorders and healthy controls. Schizophr Bull. 2023;49:1518–29.
78. Hawco C, Buchanan RW, Calarco N, Mulsant BH, Viviano JD, Dickie EW, et al. Separable and replicable neural strategies during social brain function in people with and without severe mental illness. Am J Psychiatry. 2019;176:521–30.
79. Anticevic A, Hu X, Xiao Y, Hu J, Li F, Bi F, et al. Early-course unmedicated schizophrenia patients exhibit elevated prefrontal connectivity associated with longitudinal change. J Neurosci. 2015;35:267–86.
80. Fornito A, Zalesky A, Breakspear M. The connectomics of brain disorders. Nat Rev Neurosci. 2015;16:159–72.
81. Gallucci J, Secara MT, Chen O, Oliver LD, Jones BDM, Marawi T, et al. A systematic review of structural and functional magnetic resonance imaging studies on the neurobiology of depressive symptoms in schizophrenia spectrum disorders. Schizophrenia (Heidelb). 2024;10:59.
82. Harvey PD, Twamley EW, Pinkham AE, Depp CA, Patterson TL. Depression in schizophrenia: Associations with cognition, functional capacity, everyday functioning, and self-assessment. Schizophr Bull. 2017;43:575–82.
83. Fang Z, Lynn E, Knott VJ, Jaworska N. Functional connectivity profiles in remitted depression and their relation to ruminative thinking. NeuroImage Clin. 2025;45:103716.
84. Mehta UM, Thirthalli J, Subbakrishna DK, Gangadhar BN, Eack SM, Keshavan MS. Social and neuro-cognition as distinct cognitive factors in schizophrenia: a systematic review. Schizophr Res. 2013;148:3–11.
85. Sergi MJ, Rassovsky Y, Widmark C, Reist C, Erhart S, Braff DL, et al. Social cognition in schizophrenia: relationships with neurocognition and negative symptoms. Schizophr Res. 2007;90:316–24.
86. Cohen JR, D'Esposito M. The Segregation and Integration of Distinct Brain Networks and Their Relationship to Cognition. J Neurosci. 2016;36:12083–94.
87. Jimenez AM, Riedel P, Lee J, Reavis EA, Green MF. Linking resting-state networks and social cognition in schizophrenia and bipolar disorder. Hum Brain Mapp. 2019;40:4703–15.
88. Yu J-C, Hawco C, Bassman L, Oliver LD, Argyelan M, Gold JM, et al. Multivariate association between functional connectivity gradients and cognition in Schizophrenia Spectrum Disorders. Biol Psychiatry Cogn Neurosci Neuroimaging. 2024;10:833–45. https://doi.org/10.1016/j.bpsc.2024.09.001.
89. Cheng W, Palaniyappan L, Li M, Kendrick KM, Zhang J, Luo Q, et al. Voxel-based, brain-wide association study of aberrant functional connectivity in schizophrenia implicates thalamocortical circuitry. NPJ Schizophr. 2015;1:15016.
90. Giraldo-Chica M, Woodward ND. Review of thalamocortical resting-state fMRI studies in schizophrenia. Schizophr Res. 2017;180:58–63.
91. Bernard JA, Goen JRM, Maldonado T. A case for motor network contributions to schizophrenia symptoms: evidence from resting-state connectivity. Hum Brain Mapp. 2017;38:4535–45.
92. Kaufmann T, Skåtun KC, Alnæs D, Doan NT, Duff EP, Tønnesen S, et al. Disintegration of sensorimotor brain networks in schizophrenia. Schizophr Bull. 2015;41:1326–35.
93. McCleery A, Wynn JK, Lee J, Reavis EA, Ventura J, Subotnik KL, et al. Early visual processing is associated with social cognitive performance in recent-onset schizophrenia. Front Psychiatry. 2020;11:823.
94. Javitt DC, Freedman R. Sensory processing dysfunction in the personal experience and neuronal machinery of schizophrenia. Am J Psychiatry. 2015;172:17–31.
95. Smith SM, Nichols TE, Vidaurre D, Winkler AM, Behrens TEJ, Glasser MF, et al. A positive-negative mode of population covariation links brain connectivity, demographics and behavior. Nat Neurosci. 2015;18:1565–7.
96. Finn ES, Shen X, Scheinost D, Rosenberg MD, Huang J, Chun MM, et al. Functional connectome fingerprinting: identifying individuals using patterns of brain connectivity. Nat Neurosci. 2015;18:1664–71.
97. Hsu W-T, Rosenberg MD, Scheinost D, Constable RT, Chun MM. Resting-state functional connectivity predicts neuroticism and extraversion in novel individuals. Soc Cogn Affect Neurosci. 2018;13:224–32.
98. Dosenbach NUF, Nardos B, Cohen AL, Fair DA, Power JD, Church JA, et al. Prediction of individual brain maturity using fMRI. Science. 2010;329:1358–61.
99. Nielsen AN, Greene DJ, Gratton C, Dosenbach NUF, Petersen SE, Schlaggar BL. Evaluating the prediction of brain maturity from functional connectivity after motion artifact denoising. Cereb Cortex. 2019;29:2455–69.
100. Neubauer AC, Fink A. Intelligence and neural efficiency. Neurosci Biobehav Rev. 2009;33:1004–23.
101. Ng J, Yu J-C, Feusner JD, Hawco C. Higher general intelligence is associated with stable, efficient, and typical dynamic functional brain connectivity patterns. Imaging Neuroscience. 2024;2:1–34.
102. Ebisch SJH, Gallese V, Salone A, Martinotti G, di Iorio G, Mantini D, et al. Disrupted relationship between "resting state" connectivity and task-evoked activity during social perception in schizophrenia. Schizophr Res. 2018;193:370–6.
103. Zhao W, Makowski C, Hagler DJ, Garavan HP, Thompson WK, Greene DJ, et al. Task fMRI paradigms may capture more behaviorally relevant information than resting-state functional connectivity. Neuroimage. 2023;270:119946.
104. Haddad C, Salameh P, Sacre H, Clément J-P, Calvet B. Effects of antipsychotic and anticholinergic medications on cognition in chronic patients with schizophrenia. BMC Psychiatry. 2023;23:61.
105. MacKenzie NE, Kowalchuk C, Agarwal SM, Costa-Dookhan KA, Caravaggio F, Gerretsen P, et al. Antipsychotics, metabolic adverse effects, and cognitive function in schizophrenia. Front Psychiatry. 2018;9:622.
106. Irani F, Kalkstein S, Moberg EA, Moberg PJ. Neuropsychological performance in older patients with schizophrenia: a meta-analysis of cross-sectional and longitudinal studies. Schizophr Bull. 2011;37:1318–26.
107. Park SH, Kim T, Ha M, Moon S-Y, Lho SK, Kim M, et al. Intrinsic cerebellar functional connectivity of social cognition and theory of mind in first-episode psychosis patients. NPJ Schizophr. 2021;7:59.
108. Brady RO Jr, Beermann A, Nye M, Eack SM, Mesholam-Gately R, et al. Cerebellar-Cortical connectivity is linked to social cognition trans-diagnostically. Front Psychiatry. 2020;11:573002.

109. Kent J, Pinkham A. Cerebral and cerebellar correlates of social cognitive impairment in schizophrenia. Prog Neuropsychopharmacol Biol Psychiatry. 2024;128:110850.
110. Abdi H, Williams LJ. Principal component analysis. Wiley Interdiscip Rev Comput Stat. 2010;2:433–59.

ACKNOWLEDGEMENTS

The authors would like to thank all participants for their contribution to this work, the research staff who performed data collection and management, and members of the SPINS Group.

AUTHOR CONTRIBUTIONS

Study Conceptualization: LDO, CH, ANV, RWB, AKM; Methodology: LDO, J-CY, CH, NC, ANV; Data Curation: LDO, VT; Data Analysis: LDO; Supervision: ANV; Writing, Reviewing, and Editing: LDO, J-CY, CH, NC, VT, IM-E, SXT, JMG, GF, PD, MA, RWB, AKM, ANV. All authors have read and approved the final version of the manuscript.

FUNDING

This work was supported by National Institute of Mental Health grants 1/3R01MH102324–01 (to Dr. Voineskos), 2/3R01MH102313–01 (to Dr. Malhotra), and 3/3R01MH102318–01 (to Dr. Buchanan).

COMPETING INTERESTS

LDO receives grant support from the Brain & Behavior Research Foundation (BBRF). J-CY receives grant support from the Discovery Fund of the Centre for Addiction and Mental Health (CAMH). CH receives grant support from the National Institute of Mental Health (NIMH), Canadian Institutes of Health Research (CIHR), Labatt Family Innovation Fund in Brain Health at the University of Toronto, the Natural Sciences and Engineering Research Council (NSERC), and the CAMH Foundation. NC has no conflict of interest to declare. IM-E was supported by the Labatt Family Network for Research on the Biology of Depression. SXT receives grant support from the NIMH (K23 MH130750, R21 AG082054). SXT also owns equity and serves on the board and as a consultant for North Shore Therapeutics, received research funding and serves as a consultant for Winterlight Labs, is on the advisory board and owns equity for Psyrin, and serves as a consultant for Catholic Charities Neighborhood Services and LB Pharmaceuticals. JMG has no conflict of interest to declare. GF currently receives funding from CIHR, the CAMH Foundation, and the University of Toronto. MA reported no biomedical financial interests or potential conflicts of interest. RWB has served on the Data Safety and Monitoring Boards of Roche, Merck, and Newron, and has served on the Advisory Boards of Merck, Acadia, Karuna, and Neurocrine. AKM receives grant support from the NIMH, Breakthrough Discoveries for thriving with Bipolar Disorder (BD2), and the Wellcome Trust. ANV currently receives funding from the NIMH (1/3R01 MH102324, 1/5R01 MH114970), CIHR, Canada Foundation for Innovation, CAMH Foundation, and University of Toronto.

ETHICS APPROVAL AND CONSENT

All participants signed an informed consent agreement and the protocol was approved by the respective research ethics and institutional review boards at the Centre for Addiction and Mental Health (CAMH), Zucker Hillside Hospital (ZHH), and the Maryland Psychiatric Research Center (MPRC). All research was conducted in accordance with the Declaration of Helsinki.

ADDITIONAL INFORMATION

Supplementary information The online version contains supplementary material available at https://doi.org/10.1038/s41380-026-03504-8.

Correspondence and requests for materials should be addressed to Aristotle N. Voineskos.

AND THE SPINS GROUP

William T. Carpenter[9], Jennifer Zaranski[9], Eric Arbach[9], Sharon August[9], Peter Kochunov[9], Peter Kingsley[6], Xiangzhi Zhou[6], Philipp Homan[6], Sofia Chavez[1], Gary Remington[1], Judy Kwan[1], Christina Plagiannakos[1], Mikko Mason[1], Marzena Boczulak[1], Dielle Miranda[1], Jessica Turner[11], Marco Iacoboni[12] and Michael Green[12]

[11]Department of Psychiatry and Behavioral Health, Ohio State University, Columbus, OH, USA. [12]Psychiatry and Biobehavioral Sciences, University of California, Los Angeles, Los Angeles, CA, USA.